Cumulus Transports in a Tropical Wave Composite for Phase III of GATE

RICHARD H. JOHNSON[1]

National Hurricane and Experimental Meteorology Laboratory, NOAA, Coral Gables, Fla. 33124

(Manuscript received 12 August 1977, in final form 28 October 1977)

ABSTRACT

A diagnostic study has been carried out of convective transports in tropical African wave disturbances that occurred during GATE. Data from the Reed *et al.* (1977) three-dimensional composite of eight wave disturbances during Phase III of GATE have been used in the analysis. In the compositing procedure the wave trough has been defined as the position of maximum relative vorticity at 700 mb, and eight categories in the east–west direction and seven latitude bands (separated by 4° latitude) have been assigned based on this center. The wave composite combines data from both ocean and land regions. Precipitation observations for the wave are compared to precipitation rates given by the cloud layer model to determine the magnitudes of the cumulus updraft and downdraft mass fluxes.

The findings for the innermost latitude bands confirm results from earlier studies that downdraft mass fluxes are significant in regions of deep tropical convection. In the most active categories of the wave the magnitude of the downdraft mass flux at cloud base is found to be as great as two-thirds the magnitude of the updraft mass flux at cloud base. Important meridional differences in the response of deep convection to large-scale forcing (low-level convergence) have been found. At and north of the central latitude band (11.5°N) the maximum deep cloud activity occurs about 10–20 h after the maximum low-level convergence, whereas to the south the response of deep clouds to large-scale forcing is nearly instantaneous. These differences are explained in terms of the meridional variation in the mean moisture stratification. The important role of shallow trade wind cumuli in moistening the lower troposphere in advance of the trough region at the central latitude is discussed.

1. Introduction

The diagnostic determination of cumulus transports in tropical convective systems has received considerable attention in recent years. Extensive upper air observations obtained during the 1974 GARP Atlantic Tropical Experiment (GATE) have provided an excellent data base for application of diagnostic models to study the interaction of cumulus convection with the large-scale circulation. Although at least one diagnostic study of convective systems during GATE has been completed (Nitta, 1977), determination of convective transports for a composite of the GATE African wave disturbances has not yet been reported. The first tropical wave composite for GATE (Burpee, 1975) included waves that existed during all three phases of the experiment. Reed *et al.* (1977) have prepared a three-dimensional tropical wave composite from a series of eight wave disturbances observed during Phase III of GATE. These waves, which have a maximum amplitude near 650 mb, exhibit a well-defined east-west variation of convective activity, suggesting an important degree of synoptic-scale control to the convection. In this study the diagnostic model of Johnson (1976) is used to determine the convective properties of this composite wave and to examine the control of convective updraft and downdraft activity by the large-scale flow.

A number of previous diagnostic studies of convective heat and moisture transports within tropical disturbances have been carried out that use simple one-dimensional models for the cumulus cloud (Yanai *et al.*, 1973; Ogura and Cho, 1973; Nitta, 1975). In a study based on data from the Reed and Recker (1971) composite easterly wave in the tropical western Pacific, Cho and Ogura (1974) determined that the intensities of deep and shallow cloud activity are controlled by different processes. While shallow cloud activity was found to be independent of large-scale low-level convergence, the deep cloud mass flux was found to be directly proportional to the convergence with a time lag of about 15 h. Thus, their results indicate that the response of deep clouds to large-scale forcing is not instantaneous, but rather an adjustment period is necessary before the maximum convective activity is attained. Cho (1976) indicated that during the period when the deep cloud activity is increasing there is a marked increase in the moisture content of the lower atmosphere. Conceivably, this moistening may be ac-

[1] Present affiliation: Atmospheric Sciences, University of Wisconsin, Milwaukee 53201.

complished by a deepening trade wind cumulus layer or an increasing population of shallow to moderately deep cumuli, or both.

A study by Johnson (1976) that includes effects of convective-scale precipitation downdrafts indicates that the population of shallow cumuli given by diagnostic models will be overestimated if downdrafts are neglected. This finding is supported by Nitta (1977) in a diagnostic study of cumulus updraft and downdraft transports during several convective regimes of GATE. The composite GATE tropical wave of Reed *et al.* (1977) affords the opportunity to determine convective updraft and downdraft heat and moisture transports and deep and shallow cumuli populations as a function of both longitude and latitude across the wave, an analysis which has not previously been accomplished. Particular emphasis will be given to the response of deep convective activity to large-scale forcing and the variation of this response with latitude. The moistening effects of shallow cumuli will be examined at all positions within the composite wave and an optimum determination of updraft and downdraft intensities based on the observed precipitation for the wave will be made.

2. Description of model

Since the model used in this study is identical to that described in Johnson (1976), the reader is referred to that paper for details of the development. It is an extension of the earlier work of Ogura and Cho (1973) and Nitta (1975) based on the theory of Arakawa and Schubert (1974) to include the effects of cumulus-scale precipitation downdrafts. A population of clouds is assumed to consist of cumulus elements of different sizes having updrafts and downdrafts that are modeled as one-dimensional, saturated, entraining plumes. It is assumed that updraft supplies precipitation to the downdraft; however, interactions between the two drafts are neglected. Each downdraft is assumed to originate at a level given by three-fourths the pressure-depth of the updraft and to detrain only below cloud base. An integral equation for a function representing the cloud-base mass flux for each type of cloud is solved by specifying the relative intensities of updrafts and downdrafts. The cloud model described above is admittedly crude; however, simplicity is an especially desirable feature in a model of this type, especially if it is to be incorporated into a cumulus parameterization theory (Ooyama, 1971; Arakawa and Schubert, 1974). Input parameters necessary to solve the problem include large-scale observations of wind, temperature, relative humidity and the net radiative heating rate.

To clarify discussion of results several aspects of the model need comment. The mean mass flux $\bar{M}$ ($\equiv -\bar{\omega}$), where $\bar{\omega}$ is the horizontally-averaged vertical p-velocity, is given by the sum of the net cumulus mass flux M_c and the environmental or between-cloud mass flux $\tilde{M}$, i.e.,

$$\bar{M}=M_c+\tilde{M}. \tag{1}$$

The overbar denotes an average over an area large enough to contain a statistically representative population of cumulus clouds but small compared to the large scale. M_c is given by

$$M_c=M_u+M_d, \tag{2}$$

where M_u is the updraft mass flux and M_d the downdraft mass flux. It is important to note that environmental subsidence $\tilde{M}$ depends on M_c and, thus, on the relative magnitudes of the updraft and downdraft mass fluxes, not their individual magnitudes.

Total evaporation $\bar{e}$ at each level is given by the sum of evaporation of detrained liquid water from the tops of individual updrafts $\bar{e}_u$ and the evaporation of precipitation in downdrafts $\bar{e}_d$, i.e.,

$$\bar{e}=\bar{e}_u+\bar{e}_d. \tag{3}$$

The intensity of the downdraft mass flux and, hence, the amount of evaporation that occurs in downdrafts is determined by comparing precipitation computed by the model, taking into account precipitation evaporation below cloud base, with observed precipitation (Johnson, 1976).

3. Data and computational procedures

Reed *et al.* (1977) have prepared a composite of eight tropical wave disturbances that passed over Africa and the eastern Atlantic during the period 23 August–19 September 1974. Individual waves were tracked within a region from 10°E to 31°W based on the position of the maximum relative vorticity at 700 mb, the approximate level of the maximum wave amplitude. Rawinsonde observations, surface observations, satellite IR brightness data and precipitation were composited at each synoptic hour by dividing each wave into eight columns in the east-west direction and seven rows in the north-south direction (56 rectangular areas) and assigning each observation to the appropriate area relative to the wave center. Observations over both land and ocean were combined in an energetics study for the composite wave by Norquist *et al.* (1977) and this combined data set will be used in the study here. The width of each row is 4° latitude with the central row located at 11°N over land and 12°N over the ocean. The central row will be referred to as the reference latitude at 11.5°N. Wave phases or categories for each latitude band have been numbered 1 to 8, with category 2 centered on the region of maximum northerly wind component, category 4 on the trough, category 6 on the region of maximum southerly wind and category 8 on the ridge. Categories 1, 3, 5 and 7 occupy intermediate positions. The average distance between wave categories is ~300 km or 3° latitude. Since the average wave speed was 8 m s^{-1}, the approximate

TABLE 1. Precipitation for composite wave (mm day^{-1}).

Row	Category 1	2	3	4	5	6	7	8
				Land				
+12	0	0	0.02	0.03	0	0	0	0
+8	1.76	2.44	1.59	2.50	2.19	2.41	1.87	1.83
+4	4.41	5.98	6.26	5.27	4.11	4.52	3.46	3.65
0	8.48	11.69	12.99	9.06	6.92	5.20	5.60	6.43
−4	6.50	8.33	10.14	7.09	5.52	3.91	3.57	5.14
−8	4.27	2.81	2.73	2.46	1.54	1.92	2.21	3.15
−12	0.53	0.13	0.22	0.67	0.13	0.12	0.08	0.81
				Ocean				
0	8.38	10.86	13.04	8.77	6.73	5.24	4.54	4.04
−4	11.79	14.34	15.83	12.51	9.72	5.04	4.78	7.23
−8	4.33	6.16	4.05	3.65	0.50	2.86	4.57	6.38

time interval between wave categories is 11 h, implying a total wave period of 3.5 days.

Composited values of wind, temperature, relative humidity (at 300 mb and below), geopotential height, divergence and vertical velocity at 50 mb intervals extending from the surface to 100 mb have been supplied by Reed *et al.* for use in this study. Details of the data reduction procedures and graphical displays of the above quantities may be found in Reed *et al.* (1977).

In the paper by Reed *et al.* (1977) some discussion is given concerning differences in the wave structure between land and ocean regions. The geographical distribution of observing stations is such that in addition to the major east-west variation in land and ocean observing stations within the compositing region, there is a significant north-south variation in the ratio of land to ocean observations (see their Fig. 1a and Table 1). Coastal stations have been included by Reed *et al.* with the ocean grouping of stations. From this information it is evident that wave properties at and north of the reference latitude can be considered more continental in nature than to the south (the majority of observations within the GATE A/B array fall into the latitude band centered at 7.5°N). One purpose of this paper is to emphasize important meridional differences in the wave convective transports that are thought to be related to this north-south variation in the continentality of the composite wave.

Direct observations of net radiative heating for the composite wave are not available. The significant variation in cloud cover across the wave as reported by Reed *et al.* (their Fig. 10) implies that an important variation in the IR cooling rate across the wave might exist similar to that proposed by Albrecht and Cox (1975) in a numerical study of tropical wave disturbances. Determination of realistic radiative heating rates for the composite wave based on satellite IR brightness data and their effects on diagnosed properties of cloud populations within the composite wave is in progress and will be reported on later. Model application of preliminary values of radiative heating rates for the composite wave determined from the composite cloud-cover data and data from Albrecht and Cox (1975) and Dopplick (1972) indicate that the essential results of this study will not be significantly altered from those obtained by applying constant, clear-air net radiative heating rates across the entire wave. Therefore, in this study values from Dopplick (1972) for GATE latitudes and season will be used.

Precipitation measurements for the composite wave have been presented by Reed *et al.* (see their Fig. 10b). As indicated by the authors, the reported rainfall based the GATE Quick Look Data Set appears to be excessive when compared to climatological values for this location and season. The precipitation analysis for the wave has recently been reconstructed by Reed *et al.* using later detailed 24 h rainfall data over land supplied by Lucien Finaud[2] and shipboard observations. The composited data are shown in Table 1 for both the ocean and land regions. Observations over the ocean are too few in the latitude bands north of the latitude central (row 0) to permit a reliable composite. Precipitation amounts and variations across the wave at the central latitude are nearly identical over both land and ocean. South of the central latitude, however, precipitation over the ocean exceeds that over the land by a considerable amount. The reduced amounts of rainfall over land have been attributed by Burpee (1972) to subsidence that occurs in this region of Africa that is part of a meridional circulation associated with the low-level easterly jet near 15°N. Since in this study surface and rawinsonde observations over land and ocean have been combined, the precipitation measurements used for comparison with model results will be a simple average of the values over the land and ocean.

Computations of horizontal advections of temperature and specific humidity in this analysis are based on centered differences. Vertical derivatives and interpolation of all quantities to 5 mb intervals for the solution of Eqs. (13) and (27) of Johnson (1976) are computed using a cubic spline subroutine.

4. Results

Convective transports and cloud properties have been computed for all eight categories and the inner five latitudes bands or rows. However, because of decreasing confidence in the wave structure away from the reference latitude at 11.5°N, most of the results that follow will be presented for the inner three rows. It will be seen that a sufficient description of the latitudinal variation of the wave properties is provided by analysis of the innermost central latitude bands.

[2] Agence pour la Securite de la Navigation Aerienne (ASECNA), Dakar, Senegal. Data are now part of GATE data archive, World Data Center-A, Asheville, N. C. 28801.

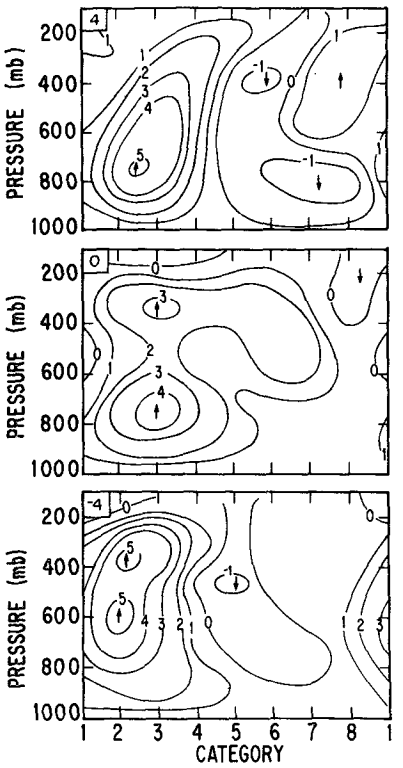

FIG. 1. The large-scale vertical motion $\bar{M}$ (mb h^{-1}) for three latitude bands of the composite wave. Numbers in upper-left portion of figures indicate latitude: 0 is the reference latitude (11.5°N) and +4 and −4 are latitude bands 4° north and south of the reference latitude (as in Reed *et al.*, 1977).

The total vertical motion field (perturbation plus zonal mean) for the inner three rows of the composite wave is shown in Fig. 1. Only the zonal mean meridional wind field enters into the computation of the zonal mean vertical velocities $\bar{M}$ because of the cyclic condition in east-west direction. Significant features of the structure in all latitudes are the low-level maxima in $\bar{M}$ from 600 to 750 mb in categories 2 and 3, well ahead of the wave trough. Recall that the trough is determined by the maximum relative vorticity at 700 mb at the reference latitude. Higher level maxima at 350 mb at and south of the reference latitude are also observed. Reed *et al.* (1977) present evidence to indicate that the larger upward motion at high levels is due to deep convection over land. Shallower convection is found to exist over the ocean. The latter finding for the GATE region is in contrast to western Pacific results (Reed and Recker, 1971) which indicate an upward motion peak near 400 mb in the wave trough region.

As a measure of the heating and moistening effects of cumulus convection, the quantities Q_1 and Q_2 were computed from large-scale observations, where

$$Q_1 \equiv \frac{\partial \bar{s}}{\partial t} + \bar{\mathbf{v}} \cdot \nabla \bar{s} + \frac{\partial}{\partial p} \bar{\omega} \bar{s}, \tag{4}$$

$$Q_2 \equiv -L\left(\frac{\partial \bar{q}}{\partial t} + \bar{\mathbf{v}} \cdot \nabla \bar{q} + \frac{\partial}{\partial p} \bar{\omega} \bar{q}\right), \tag{5}$$

where $s = c_p T + gz$ is the dry static energy, q the specific humidity and L the latent heat of condensation. These quantities are shown for the inner three rows in Figs. 2 and 3. The maximum convective heating Q_1 occurs over a broad region from categories 3 to 6 at the reference latitude with peaks near 700 and 400 mb. The heating in the regions north and south of the reference latitude is confined to narrower regions in the east-west direction with slightly greater maxima in the mid-troposphere, ~6°C day^{-1} as opposed to ~4°C day^{-1} at the reference latitude.

The apparent drying Q_2 at the reference latitude has maxima near 850 mb near category 3 and at 600 mb in category 6. North and south of the central latitude the maxima are in category 2 between 800 and 900 mb with larger peak values, ~6–8°C day^{-1}, rather than the ~4°C day^{-1} maxima at the reference latitude. The significant meridional variation in Q_1 and Q_2 leads to diagnosed cumulus mass transports that also vary significantly with latitude, as will be discussed shortly.

As mentioned earlier, determination of the updraft and downdraft intensities is based on a comparison of model-computed precipitation with observed. Evaporation below cloud base is determined by assuming that the evaporation rate at cloud base given by the cloud

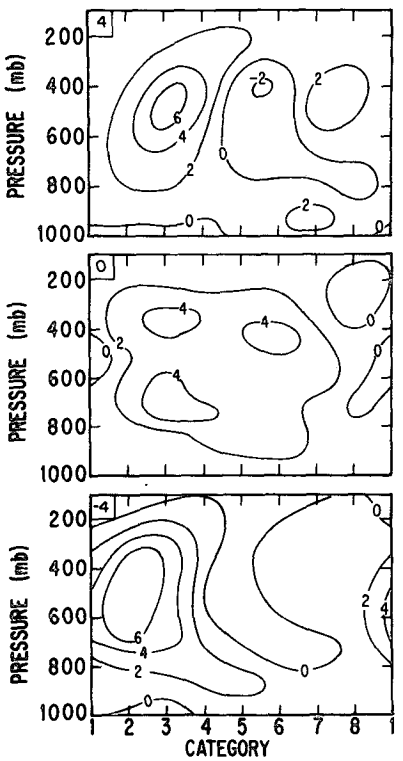

FIG. 2. The apparent heat source Q_1 (°C day^{-1}) for the three central latitude bands of the composite wave.

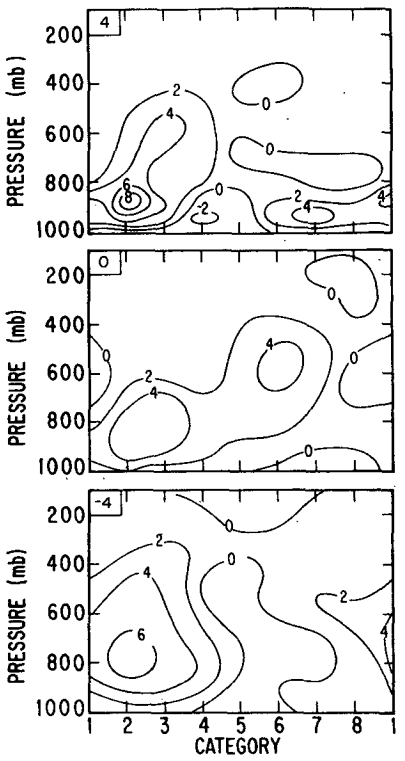

FIG. 3. The apparent moisture sink Q_2 (°C day^{-1}) for the three central latitude bands of the composite wave.

model is equal to the rate for the entire subcloud layer. Determination of the appropriate cloud base to assign to each latitude band is complicated by the fact that cloud-base levels are different over ocean and land and the data set is a mixture of land and ocean observations. The approach taken here is to have cloud base be given by the lifting condensation level of the surface air for the combined land-ocean composite wave. Accordingly, cloud bases are taken as 950 mb at 11.5, 7.5 and 3.5°N, 900 mb at 15.5°N and 850 mb at 19.5°N, assuming an average surface pressure of 1010 mb. A plot of observed precipitation and the computed rainfall rates for the central three latitude bands is shown in Fig. 4. The computed values are based on the assumption that no downdrafts exist, i.e., in terms of Johnson (1976) $\epsilon = m_0(\lambda)/m_B(\lambda) = 0$ where $m_0(\lambda)$ is the downdraft originating level mass flux per unit λ (entrainment rate) and $m_B(\lambda)$ the cloud-base mass flux per unit λ. Thus, ϵ is a measure of the downdraft intensity relative to the updraft intensity. An immediately apparent result is the finding that at all latitudes the diagnosed rainfall rates in most regions of the wave are greater than those observed when downdrafts are neglected. For the reference latitude and the latitude band to the south the precipitation rates for the wave are overestimated for $\epsilon = 0$ by 34% and 21%, respectively. Johnson (1976) found the rainfall rates to be overestimated for $\epsilon = 0$ for the Reed and Recker (1971) western Pacific composite wave mean trough position (categories 3, 4, 5; 1–2–1 smoothed) by 22%. Quantitative comparison of these values for the two different tropical regions is not warranted because of the different averages; however, it appears that at least at the reference latitude relative downdraft intensities in the wave trough in the GATE region are greater than in the western Pacific. This finding is in agreement with Nitta's (1977) comparative results of downdraft mass fluxes between the same two regions using only oceanic observations from GATE. From Fig. 4 it is evident that the greatest departures from the observed precipitation in the three regions are (from north to south) in categories 3, 6 and 2, respectively. As a result, the greatest downdraft intensities should be expected in or near these categories.

In Table 2 optimum values of ϵ (values for which computed precipitation equals observed) at the reference latitude and the adjacent region to the south are shown. In three of the categories (indicated by asterisks) agreement between computed and observed precipitation was not achieved for a positive value of the total evaporation of detrained liquid water from up-

TABLE 2. Optimum values of ϵ. Values indicated by asterisks are for $E_u = 0$.

Row	Category 1	2	3	4	5	6	7	8
0	0	0	0.16	0.31	0.49*	0.39*	0.29	0
−4	0.40	0.67*	0.39	0	0	0.09	0.21	0.15

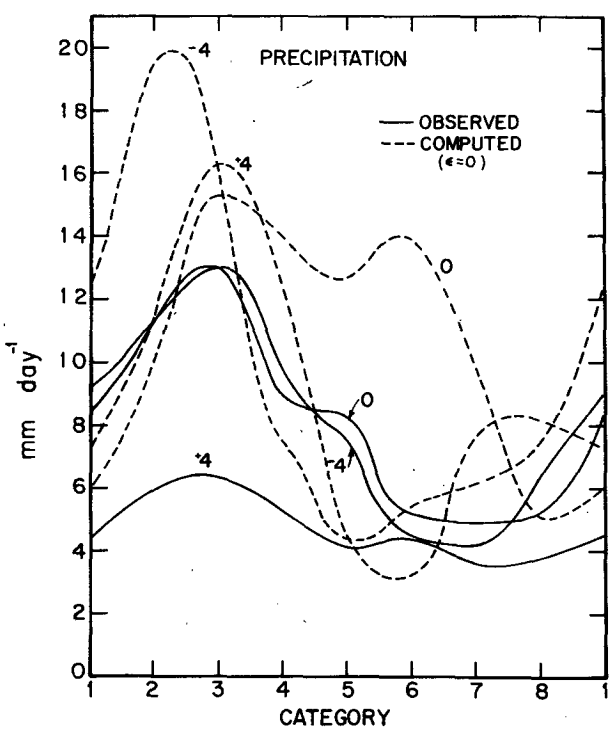

FIG. 4. Observed and computed ($\epsilon = 0$) precipitation rates for central three latitude bands of the composite wave.

drafts E_u. Here E_u is the vertical integral of $\bar{e}_u$ from cloud base to the level of the top of the deepest cloud. In these three cases ϵ was selected as that value at which $E_u=0$. No doubt deficiencies in the model and/or inadequacies of certain assumptions required for its application exist in these highly convective regions. Results for 15.5°N are not presented because difficulty was encountered in determining the lower tropospheric mass fluxes. The source of the problem is the fact that most of the observations at this latitude are over the sub-Saharan region and, consequently, the mean thermodynamic structure does not accurately represent the cloud environment; namely, it is too dry. A non-unique cloud population in the lower troposphere is found when the composite soundings are used at all latitudes north of the reference latitude. Cloud mass fluxes are not significantly affected above 500 mb, however, and some results above this level will be presented later.

At this point it is appropriate to examine the accuracy of the precipitation measurements and model sensitivity to the actual amounts. First note in Table 1 that the rainfall rates at the reference latitude are in good agreement over land and ocean: only in categories 7 and 8 do they differ by more than 10%. The use of an average of land and ocean observations for this latitude should therefore not lead to a problem of interpretation based on possible land-ocean differences. The variation of precipitation across the wave indicated in Table 1 agrees with that presented by Reed *et al.* (1977) in their Fig. 10b. It can also be noted that the general pattern of precipitation on the whole resembles the distribution of satellite-observed cloud cover (Fig. 10a, Reed *et al.*, 1977). The average rainfall rate at the reference latitude of 8.2 mm day^{-1} (from Table 1) agrees rather well with the climatological value for this region and season of 250 mm month^{-1} (e.g., Burpee, 1972). Reed *et al.* report that the earlier values, having an average of 11 mm day^{-1} at the reference latitude (used to produce their Fig. 10b), were excessive when compared to climatological data. Thus the magnitude and phase of the precipitation rates used in this paper at the reference latitude appear reasonable. The sensitivity of the model to errors in precipitation amounts is such that a 20% error in the rainfall rate will change the diagnosed optimum value of ϵ by 0.15.

At 7.5°N there is obviously a large disparity between the land and ocean precipitation rates. While significant differences in optimum ϵ result from the separate application of the land and ocean values, both results yield a maximum ϵ in category 2 (as in Table 2 for the average). Therefore, the qualitative conclusion that the maximum relative downdraft intensity occurs in category 2 at 7.5°N should not be affected by the averaging procedure that has been adopted.

There exists independent evidence to support the contention here that ϵ and, hence, downdraft activity

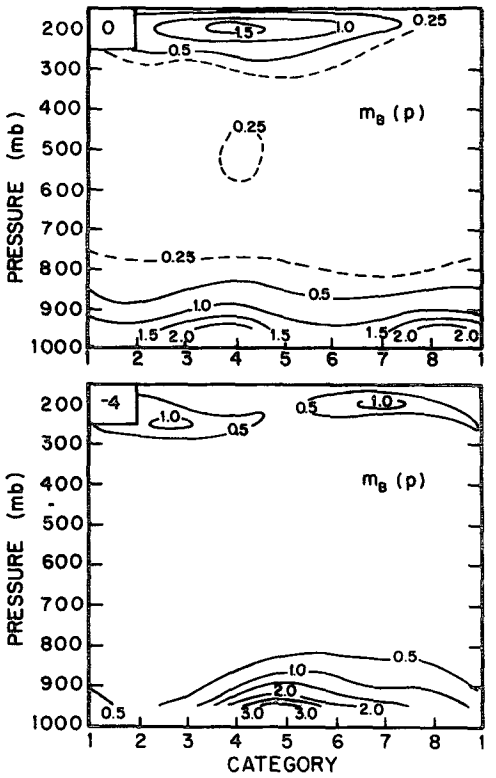

FIG. 5. The cloud-base mass flux $m_B(p)$ (day^{-1}) per unit interval of cloud-depth for the reference latitude and 4° to the south.

may vary significantly across the wave. Using a somewhat different approach the GATE study of Nitta (1977) has shown that the intensity of downdrafts in relation to updrafts can vary by an important degree from one convective regime to another over a time scale of about 12 h.

The solution for the cloud base mass flux $m_B(p)$ per unit interval of cloud depth is shown for the reference latitude and 4° to the south in Fig. 5. The bimodal distribution of cloud sizes reported earlier for other tropical regions (Yanai *et al.*, 1973; Ogura and Cho, 1973; Nitta, 1977) is clearly evident in most portions of the wave. Notably, however, only a single peak is present at 7.5°N in the region of the wave containing the most intense downdrafts (Table 2 and Fig. 6). Johnson (1976) earlier pointed out the effects of downdrafts in reducing the diagnosed population of shallow cumuli in deep convective regimes. The reduction in $m_B(p)$ in the lower troposphere in the strong downdraft region at 11.5°N is not nearly as pronounced as that which occurs at 7.5°N. The existence of shallow cumulus clouds in advance of the wave trough at the reference latitude will be examined in the following discussions. The peak in $m_B(p)$ near 200 mb in category 7 at 7.5°N indicates that deep cloud activity also exists in the ridge at this latitude in contrast to the single upper tropospheric peak at the central latitude. The composite cloudiness results shown by Reed *et al.* (1977) do not indicate a secondary

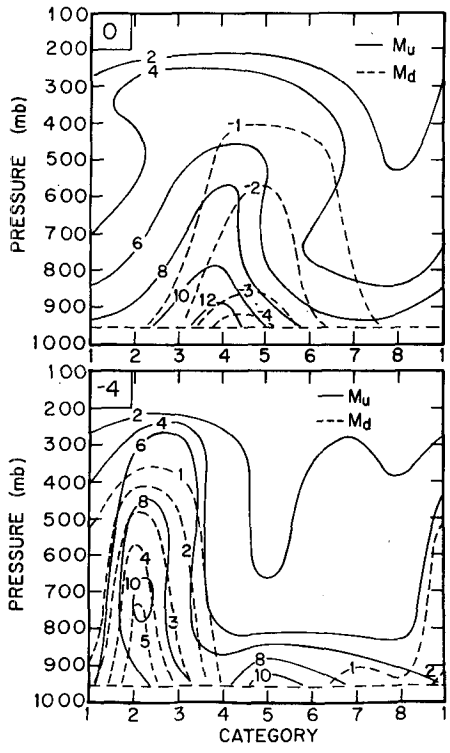

FIG. 6. Updraft and downdraft mass fluxes M_u and M_d (mb h^{-1}) at and to the south of the reference latitude.

maximum in cloud cover near the ridge, so this feature may not be real.

The updraft and downdraft mass fluxes at 11.5 and 7.5°N are shown in Fig. 6. There are several significant differences between the two latitudes. When considering these differences, it should be kept in mind that these data are for the combined ocean and land areas and that there exists a meridional variation in the ratio of land to ocean observations within this region of the composite wave, as discussed earlier. At the reference latitude the updraft mass flux M_u has a broad maximum with largest values near category 4. The peak downdraft mass flux occurs 10–15 h later near category 5. At 7.5°N, on the other hand, a very narrow maximum in M_u occurs between categories 2 and 3 with a nearly coincident peak in M_d. At both latitudes downdraft activity is mainly associated with deep cumulus activity, but as indicated, the phase relationships between M_u and M_d differ. The causes of this meridional difference in the phases are difficult at this stage to determine. They may be related to the large-scale vertical wind shear, thermodynamic stratification, some combination of both or, possibly, to the lifetime characteristics of the cloud clusters associated with the waves. The lifetimes of the clusters may well be controlled by processes on the mesoscale or even smaller scales.

To further explore the meridional variation in the wave structure the response of deep cumulus clouds to large-scale forcing is examined. In Fig. 7 the large-scale subcloud layer convergence, given in terms of the mean 950 mb mass flux, $\bar{M}_{950}$, and the mass flux M_{CD} at cloud base due to clouds with tops above 500 mb (identical to that defined by Cho and Ogura, 1974) are plotted for all portions of the composite wave. In this study we choose to define large-scale forcing in terms of low-level convergence $\bar{M}_{950}$ because of the frequent application of this concept in wave-CISK studies (e.g., Hayashi, 1970; Lindzen, 1974). Certainly deep cumulus activity may be correlated to the vertical motion field at higher levels as Yanai *et al.* (1976) indicate; however, vertical motion at higher levels in tropical disturbances is most likely a consequence of the deep convection rather than a cause. At and north of the reference latitude the maximum low-level convergence occurs from 11 to 20 h before the maximum deep cumulus mass flux. This finding is consistent with results of Cho and Ogura (1974) who found a peak in M_{CD} 15 h after the maximum $\bar{M}_{950}$ for the western Pacific Reed and Recker (1971) wave composite which was centered near 9°N. South of the reference latitude, however, the $\bar{M}_{950}$ and M_{CD} peaks are nearly coincident. Apparently in this near equatorial region deep cumulus activity responds nearly instantaneously to the large-scale forcing.

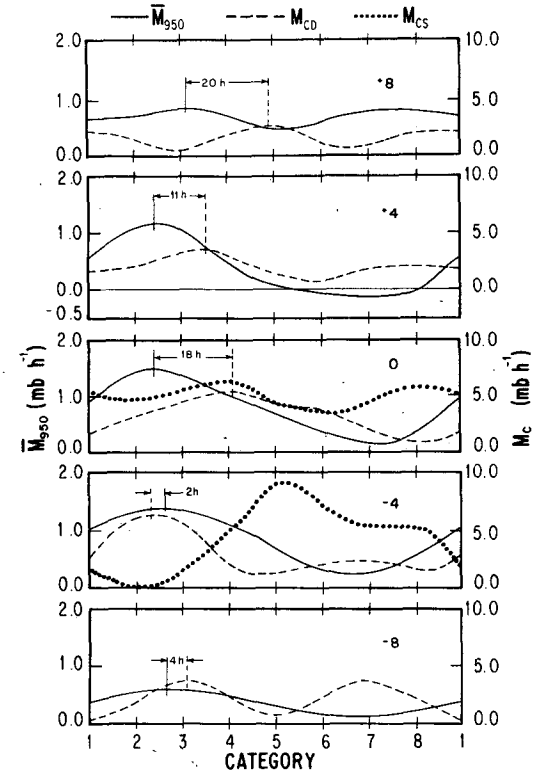

FIG. 7. The large-scale 950 mb mass flux $\bar{M}_{950}$, cumulus mass flux M_{CD} due only to clouds with tops above 500 mb and cumulus mass flux M_{CS} due only to clouds with tops below 750 mb. Solid (dashed) vertical lines at wave crests indicate positions of maximum $\bar{M}_{950}$ (M_{CD}). Time intervals between maxima are indicated. M_{CS} is shown only at 0, −4 latitude bands.

A possible explanation for the meridional variation in the response of deep cloud activity to large-scale forcing is evident if the relative humidity structure for the entire wave is examined (Fig. 8). In the two southern regions a deep moist layer is evident with only a minor variation across the wave. To the north, however, at the time of maximum large-scale forcing (indicated by the solid arrows) the lower troposphere is not as moist as it is in the southern regions. From the time of maximum $\bar{M}_{950}$ to the time of maximum M_{CD} the lower troposphere experiences significant moistening. This moistening is most likely achieved through an increasing population of shallow cumulus clouds which detrain water vapor and liquid water in the mid-to lower troposphere. Fig. 9 shows the detrainment moistening increasing at 11.5°N from category 2 to a maximum in category 4. The following moisture balance equation has been used here:

$$\frac{-Q_2}{L} = -(M_u+M_d)\frac{\partial \tilde{q}}{\partial p}+\delta(q_u-\tilde{q})+\bar{e}_u, \qquad (6)$$

where δ is the detrainment rate, q_u the specific humidity

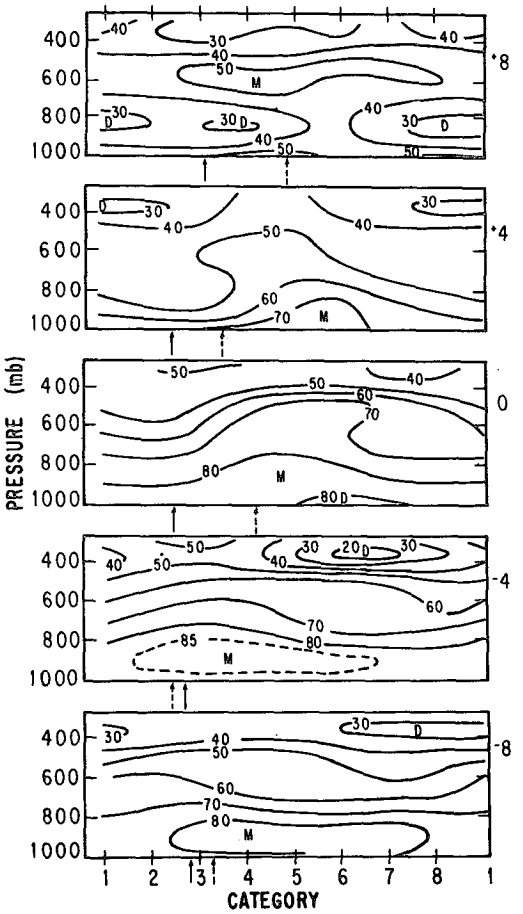

FIG. 8. Relative humidity (%) for the composite wave. Solid (dashed) arrows indicate positions of maximum $\bar{M}_{950}$ (M_{CD}).

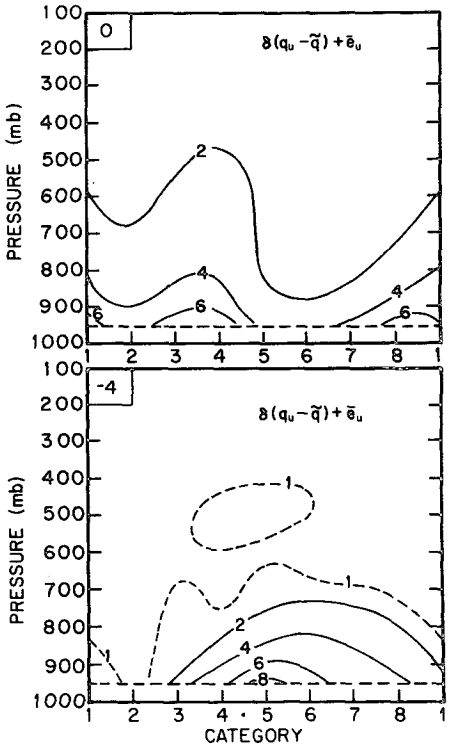

FIG. 9. Detrainment of water vapor and evaporation of detrained liquid water at and to the south of the reference latitude. Units: g kg^{-1} day^{-1}.

at the top of updrafts and $\tilde{q}$ the environmental specific humidity. When the lower troposphere is sufficiently moistened by this process, then the maximum deep cloud activity can occur. A similar process on smaller space scales and time scales has been described as occurring in the development of sea breeze convection over the south Florida peninsula by Johnson (1977). At 7.5°N detrainment moistening is greatest approximately one day after the period of most intense deep cumulus activity (Fig. 9). The moistening is a result of trade wind cumuli that exist in the undisturbed regions of the wave. These clouds serve to restore the atmosphere to its mean conditionally unstable state following the strong vertical mixing of moist static energy by updrafts and downdrafts that occurs earlier.

Cho and Ogura (1974) found no apparent relationship of the shallow cumulus activity to large-scale forcing. Since downdrafts were not considered in their model and inclusion of their effects reduces the shallow cumulus population (Johnson, 1976), it is important to reexamine this problem. In Fig. 7 the cloud base mass flux M_{CS} due only to shallow or trade wind cumuli, those with tops below 750 mb, is plotted at 11.5°N and 7.5°N. We first note that at 7.5°N M_{CS} is nearly 180° out of phase with M_{CD}. When the deep cloud mass flux is greatest, there is a minimum in shallow cumulus activity. Conversely, when there is a minimum of deep cloud activity, the shallow trade wind cumulus mass

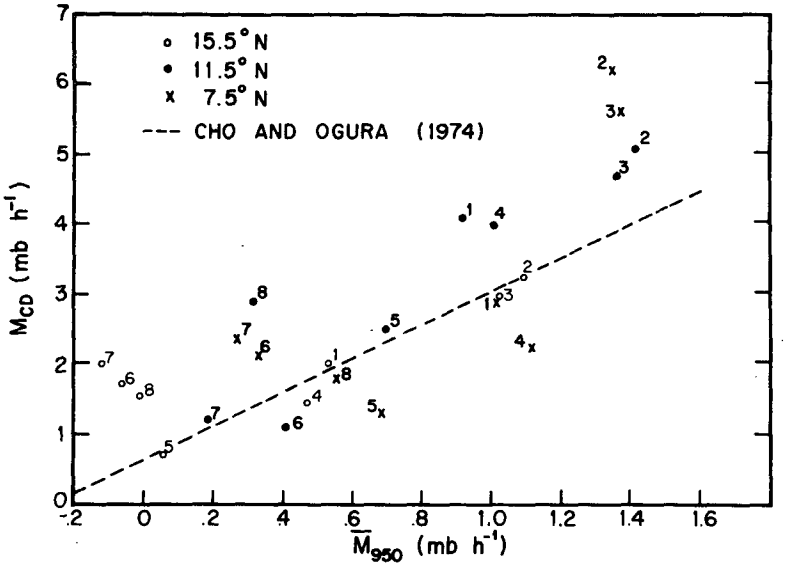

FIG. 10. Deep cumulus mass flux M_{CD} as a function of the large-scale low-level convergence $\bar{M}_{950}$ shifted in time according to the phase differences shown in Fig. 7. Numbers indicate wave categories.

flux is greatest. At 11.5°N, however, the maximum in M_{CS} coincides with the maximum in M_{CD}, although there is a secondary maximum in M_{CS} at the position of the minimum in M_{CD}. The results at 7.5°N suggest that shallow cumulus activity is significantly suppressed in the region of deep cumulus activity, presumably as a result of downdraft stabilization of the subcloud layer (Garstang, 1967; Zipser, 1969). Mandics and Hall (1976) present acoustic sounder data obtained during Phase III of GATE that clearly indicate the stabilizing effects of downdrafts on the lower boundary layer. They note that modifications of the boundary layer caused by cumulus downdrafts typically lasted for 5–6 h, whereas those due to squall lines persisted for 12–16 h. Houze (1977) presents similar evidence of low-level stabilization following the passage of a squall-line system during Phase III. Figs. 5, 7 and 9 show that about a day after the deep convection, the trade wind cumulus field is restored. By way of contrast, at 11.5°N M_{CS} increases concurrently with M_{CD} ahead of the wave trough, indicating that both deep and shallow clouds are responding to the large-scale forcing. The enhanced shallow cumulus activity, which moistens the lower troposphere (Fig. 9), is apparently a prerequisite for the growth of deep clouds at this latitude. The existence of a maximum in M_{CS} in the wave trough, however, is not readily explainable considering the stabilizing effects of downdrafts that likely exist in this region. This feature may not be realistic. At present observational evidence to support this result is not available. Significant shallow cumuli mass fluxes also exist in the ridge region, as mentioned earlier.

The results shown in Fig. 7 for the three inner rows indicate a strong relationship between $\bar{M}_{950}$ and M_{CD}. A plot has been prepared of M_{CD} as a function of $\bar{M}_{950}$ (Fig. 10) where the values of $\bar{M}_{950}$ have been adjusted by +11, +18, and −2 h at 15.5, 11.5, and 7.5°N, respectively, according to the phase differences shown in Fig. 7. Fig. 10 also contains results obtained by Cho and Ogura (1974) using the western Pacific data of Reed and Recker (1971). The geographical area of a wave category in both the Pacific and GATE regions is approximately the same. While Cho and Ogura found an approximate linear relationship in their analysis, the results of this study for the GATE region do not clearly indicate a particular functional form for the relationship between M_{CD} and $\bar{M}_{950}$. For $\bar{M}_{950} \lesssim 0.8$ mb h^{-1} M_{CD} appears to be independent of $\bar{M}_{950}$, whereas for $\bar{M}_{950} > 0.8$ mb h^{-1}, M_{CD} is definitely an increasing function of $\bar{M}_{950}$. The positive M_{CD} for no large-scale forcing ($\bar{M}_{950}=0$) is indicative of the background deep cumulus activity that exists primarily to offset upper tropospheric radiational heat losses.

The determination of a precise relationship between deep cumulus activity and large-scale forcing within the composite African wave has likely been complicated by the fact that the data over land and ocean regions have been combined in our analysis here. Further clarification of this important problem will probably have to await analyses of data for land and ocean areas separately where tropospheric and boundary layer structures are treated separately rather than averaged. Additional studies in this area are encouraged.

We present finally the net cumulus mass flux M_c (Fig. 11) and the environmental mass flux $\tilde{M}$ (Fig. 12) at 11.5 and 7.5°N. As found in the western Pacific (Johnson, 1976; Nitta, 1977) and in the GATE region by Nitta (1977) it is seen that downdrafts reduce M_c

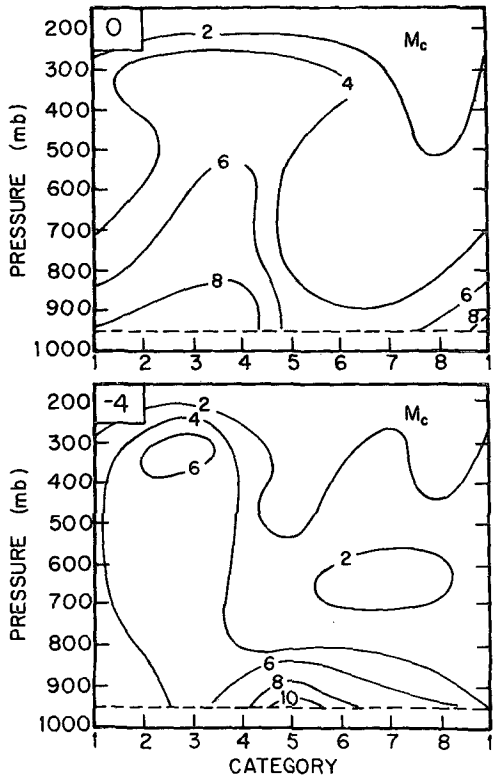

FIG. 11. The net cumulus mass flux M_c (mb h^{-1}) at and south of the reference latitude.

considerably below M_u in the lower troposphere in the deep convective portions of the wave (cf. Fig. 6). As a result $\tilde{M}$ in these regions is less in the lower troposphere (Fig. 12) than it would be if downdrafts had not been included. Nitta (1977) found very little variation in $\tilde{M}$ with the intensity of convective activity. Our results indicate, however, that $\tilde{M}$ does vary considerably across the wave, being greatest in the regions of largest shallow cumulus mass flux (cf. Figs. 7 and 12). The large environmental subsidence near cloud base centered near category 5 at 7.5°N and in categories 1–3 at 11.5°N is accounted for mostly by shallow or trade wind cumulus clouds in these regions having little or no organized downdrafts so that the compensating downward motion to the shallow updrafts occurs almost exclusively in the cloud environment. Of course, one would expect nonprecipitating shallow cumuli in all portions of the wave to have little or no organized downdrafts. The assumption of large ϵ for shallow clouds in disturbed regions is not reasonable, but the contributions from deep cloud downdrafts dominate M_d in these regions so that the effect of this assumption on the results is not significant (tests of this effect have been carried out). In the region of greatest deep convection at 7.5°N $\tilde{M}$ is small at all levels, i.e., $M_c \approx \tilde{M}$ above about 800 mb.

5. Summary and concluding remarks

In this study convective transports within the composite African wave disturbance of Reed *et al.* (1977) for Phase III of GATE have been determined using a diagnostic model that includes effects of cumulus updrafts, downdrafts and precipitation evaporation. At the central latitude band of the composite wave, 11.5°N, the maximum deep cumulus updraft mass flux has been found to occur about one-half day before the maximum downdraft mass flux. At 7.5°N, on the other hand, the maximum updraft and downdraft mass fluxes are nearly coincident. The same phase relationships also exist between deep cumulus mass flux and large-scale low-level convergence with the low-level convergence preceding the deep cumulus mass flux at and north of 11.5°N by ~10–20 h. These meridional differences in the cumulus mass transports are explained in terms of the meridional differences in the mean moisture stratification. Increasing populations of shallow cumuli that are found preceding the wave trough at 11.5°N serve to moisten the lower troposphere in advance of the deep convection that follows. At 7.5°N, however, shallow cumuli are noticeably absent in the region of greatest deep convective activity, presumably as a result of the stabilizing influence of strong cumulus downdrafts.

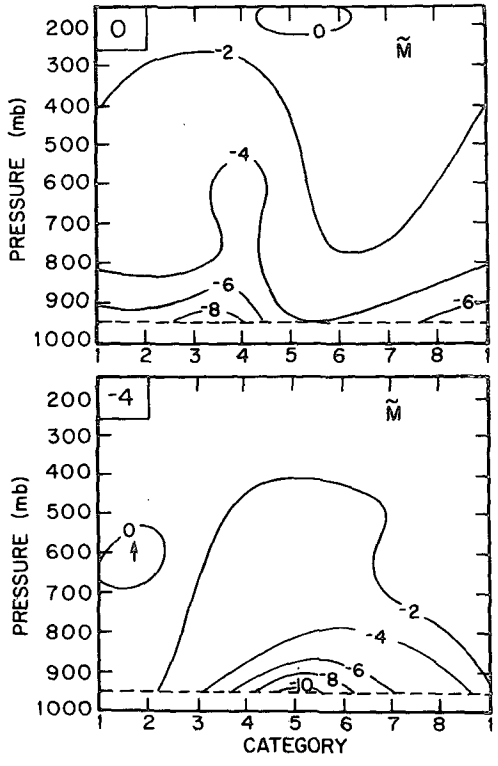

FIG. 12. The environmental subsidence $\tilde{M}$ (mb h^{-1}) at and south of the reference latitude.

The fact that deep cumulus activity does not respond instantaneously to low-level convergence at some tropical latitudes has a direct implication for wave-CISK theories. In particular, the amplitude and vertical distribution of diabatic heating associated with convection may not necessarily be specified independently of the thermodynamic stratification. In regions away from the very moist equatorial zones the maximum convective heating by deep clouds is apparently realized nearly one-half day or so following the maximum low-level convergence.

In summary, results of this investigation indicate that significant meridional differences in the convective mass flux properties of the Reed *et al.* composite wave exist. Further, the intensity of deep cumulus activity appears to be directly related to the magnitude of the large-scale low-level convergence only when the convergence exceeds a certain level. While these findings are felt to be qualitatively correct, further similar studies with the final GATE data sets over the separate ocean and land regions will be required before more detailed questions can be answered concerning the forcing of cumulus activity by larger scales of motion. The success of such studies will depend in a large part on the accuracy of the rawinsonde observations and rainfall measurements obtained during GATE.

Acknowledgments. I express appreciation to Prof. Richard J. Reed of the University of Washington for providing the tropical wave composite data used in this study. I would also like to thank Dr. Robert Burpee for several helpful comments on the paper.

REFERENCES

Albrecht, B., and S. K. Cox, 1975: The large-scale response of the tropical atmosphere to cloud-modulated infrared heating. *J. Atmos. Sci.*, **32**, 16–24.

Arakawa, A., and W. Schubert, 1974: Interaction of cumulus cloud ensemble with the large-scale environment, Part I. *J. Atmos. Sci.*, **31**, 674–701.

Burpee, R. W., 1972: The origin and structure of easterly waves in the lower troposphere of North Africa. *J. Atmos. Sci.*, **29**, 77–90.

——, 1975: Some features of synoptic-scale waves based on compositing analysis of GATE data. *Mon. Wea. Rev.*, **103**, 921–925.

Cho, H. R., 1976: Effects of cumulus cloud activity on the large-scale moisture distribution as observed in Reed-Recker's composite easterly waves. *J. Atmos. Sci.*, **33**, 1117–1119.

——, and Y. Ogura, 1974: A relationship between cloud activity and low-level convergence as observed in Reed-Recker's composite easterly waves. *J. Atmos. Sci.*, **31**, 2058–2065.

Dopplick, T. G., 1972: Radiative heating of the global atmosphere. *J. Atmos. Sci.*, **29**, 1278–1294.

Garstang, M., 1967: Sensible and latent heat exchange in low-latitude synoptic-scale systems. *Tellus*, **19**, 492–509.

Hayashi, Y., 1970: A theory of large-scale equatorial waves generated by condensation heat and accelerating the zonal wind. *J. Meteor. Soc. Japan*, **48**, 140–160.

Houze, R. A., 1977: Structure and dynamics of a tropical squall-line system observed during GATE. *Mon. Wea. Rev.*, **105**, 1540–1567.

Johnson, R. H., 1976: The role of convective-scale precipitation downdrafts in cumulus and synoptic-scale interactions. *J. Atmos. Sci.*, **33**, 1890–1910.

——, 1977: Effects of cumulus convection on the structure and growth of the mixed layer over south Florida. *Mon. Wea. Rev.*, **105**, 1713–1724.

Lindzen, R. S., 1974: Wave-CISK in the tropics. *J. Atmos. Sci.*, **31**, 156–179.

Mandics, P. A., and F. F. Hall, Jr., 1976: Preliminary results from the GATE acoustic echo sounder. *Bull. Amer. Meteor. Soc.*, **57**, 1142–1147.

Nitta, T., 1975: Observational determination of cloud mass flux distributions. *J. Atmos. Sci.*, **32**, 73–91.

——, 1977: Response of cumulus updraft and downdraft to GATE A/B-scale motion systems. *J. Atmos. Sci.*, **34**, 1163–1186.

Norquist, C. C., E. E. Recker and R. J. Reed, 1977: The energetics of African wave disturbances as observed during Phase III of GATE. *Mon. Wea. Rev.*, **105**, 334–342.

Ogura, Y., and H. R. Cho, 1973: Diagnostic determination of cumulus cloud populations from observed large-scale variables. *J. Atmos. Sci.*, **30**, 1276–1286.

Ooyama, K., 1971: A theory on parameterization of cumulus convection. *J. Meteor. Soc. Japan*, **49**, (Special Issue), 744–756.

Reed, R. J., and E. E. Recker, 1971: Structure and properties of synoptic-scale wave disturbances in the equatorial western Pacific. *J. Atmos. Sci.*, **28**, 1117–1133.

——, D. C. Norquist and E. E. Recker, 1977: The structure and properties of African Wave Disturbances as observed during Phase III of GATE. *Mon. Wea. Rev.*, **105**, 317–333.

Yanai, M., S. Esbensen and J. H. Chu, 1973: Determination of bulk properties of tropical cloud clusters from large-scale heat and moisture budgets. *J. Atmos. Sci.*, **30**, 611–627.

——, J. H. Chu, T. E. Stark and T. Nitta, 1976: Response of deep and shallow tropical maritime cumuli to large-scale processes. *J. Atmos. Sci.*, **33**, 976–991.

Zipser, E. J., 1969: The role of organized unsaturated convective downdrafts in the structure and rapid decay of an equatorial disturbance. *J. Appl. Meteor.*, **8**, 799–814.